Crystalline and Composite Scintillators for Fast and Thermal Neutron Detection

Nikolai Z. Galunov[1,2], Natalya L. Karavaeva[1], and Oleg A. Tarasenko[1(✉)]

[1] Institute for Scintillation Materials, National Academy of Sciences of Ukraine, Kharkiv, Ukraine
tarasenko@isma.kharkov.ua
[2] V.N. Karazin Kharkiv National University, Kharkiv, Ukraine

Abstract. The control of the radioecological situation around nuclear power plants requires the detection of very low neutron fluxes. It makes necessary to use the large area detection systems. The same task is topical for radiobiology, radiomedicine, geological logging, and space applications. We proposed the technology to obtain the new class of scintillation materials, namely organic composite scintillators. It allows us to create the scintillation detectors of an unlimited area. We consider the hydrogen-bearing composite scintillators as a typical example of the detectors for fast neutrons and the composite scintillators based on grains of the Gd-bearing materials as the thermal neutron detectors. We discuss the combined detectors for selective detection of thermal and fast neutrons in the presence of background gamma radiation as well.

1 Introduction

The problem of detection of low intensity fluxes of neutrons is of a great importance in modern ecological, geological, biological, medical applications, custom survey, etc. Such a radiation is the most hazardous for human organism. The radiation-weighting factor w_R is the value expressing the long-term risk (primarily cancer, leukaemia, heavy pulmonary allergies, etc.) of a low-level chronic exposure. It depends on a radiation type and other factors. For example, for gamma radiation photons $w_R = 1$, while for fast neutrons with energies $E_n < 2$ meV, the $w_R = 20$. For thermal neutrons, $w_R = 5$ [1].

For fast neutron spectrometry of the low neutron fluxes, it is necessary to obtain a large-area non-hygroscopic cheap detector, which has a detection high efficiency and is able to effective pulse shape discrimination (PSD). The development of the effective single crystals, plastics and liquid scintillators with high PSD capability is the subject of research for more than 50 years. The PSD capability of organic single crystals, until now, is significantly higher than for liquid and plastic scintillators [2–11]. Liquid scintillators are toxic and often flammable. Thus, organic single crystals could be a very good option for fast neutron detection with their favourable characteristics, i.e., their high light yield and PSD. However, it is difficult to obtain a large area scintillator even using the modern techniques of crystal growth and they are comparatively expensive due to the stage of a crystal growth [12 (p. 25)].

M. Korzhik and A. Gektin (eds.), *Engineering of Scintillation Materials and Radiation Technologies*, Springer Proceedings in Physics 200,
https://doi.org/10.1007/978-3-319-68465-9_12

To resolve these conflicting requirements, we have recently proposed the composite scintillator as a gel composition that contains the grains of scintillation material. We obtain the organic molecular single crystal grains using grinding the boule under the layer of liquid nitrogen when it cracks at the grain boundaries. We obtained the boule in the process of purification of the raw material by orientated crystallization. It allows us to avoid growing a single crystal. It appreciably cheapens production of obtaining organic scintillation grains and the scintillator as well. We designed the technique of joining the different composite scintillators in one area. It increases the detection efficiency due to growing the detection spatial angle. A high temperature stability of the light yield of organic scintillators increases their possible use for advanced applications at high and low temperatures [13–18].

Figure 1 demonstrates the dependence of the total capture cross-section σ_{tot} of neutrons as the function of their energy E_n. Two processes determine the value of σ_{tot}. It is (i) elastic potential scattering on nuclear forces, or (ii) nuclear scattering. A distinctive feature of the first and the last of the processes is that: (i) a neutron does not penetrates inside a nucleus $(n, n)_{pot}$ and (ii) a neutron penetrates inside a nucleus. Nuclear reactions of the following types: (n, γ), (n, p), (n, α), (n, f), inelastic neutron scattering (n, n'), and elastic (resonance) neutron scattering $(n, n)_{res}$ may occur in the latter case. The values of corresponding cross-section (consequently the type of a material) determine the relative role of each the process. With the scattering cross-section value (σ_s) increase the probability of the process (i) grows but it decreases with absorption (σ_a) cross-section value increase. Therefore, the probability of the process (i) is higher when $\sigma_s > \sigma_a$ and the probability of the process (ii) is higher when $\sigma_s < \sigma_a$. Reactions of neutron radiative capture (n, γ) are effective for slow (epithermal and thermal) neutrons with the energy $E_n \sim 0.026$ eV–500 keV [12, 19].

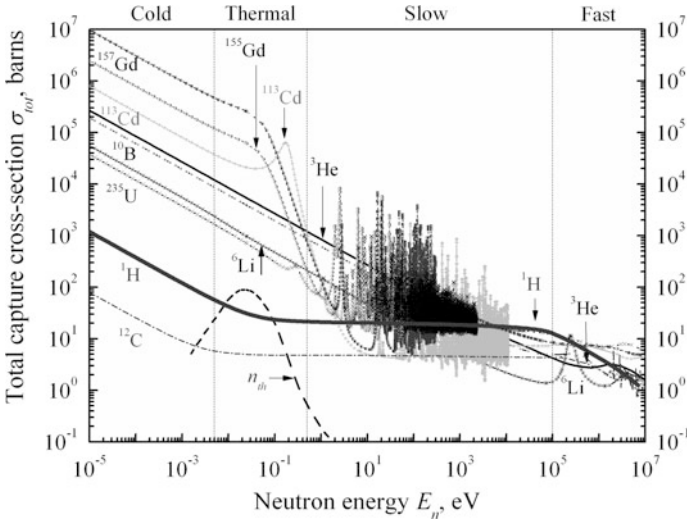

Fig. 1. Total cross-sections σ_{tot} of neutrons versus their energy E_n for some isotopes [12 (p. 401)]

The problem of thermal neutron detection by organic and inorganic materials is the subject for discussion since the late fifties and is relevant in the current investigations [5, 20, 21]. For high σ_a—values the thermal neutron path in a scintillator is significantly shorter than the penetration depth of photons of gamma radiation of middle and high-energies. Table 1 shows the characteristics of the isotopes that have a high cross-section σ_a of thermal neutron radiative capture [12 (p. 402)]. In contrast to fast neutrons, for thermal neutrons, the spectrometry is not necessary and, therefore, the resolution of the scintillation amplitude spectrum does not so important. For thermal neutrons, the separation of the signals generated by thermal neutrons and the gamma background radiations becomes the more important problem. It solution is not so simple. In the case of the thermal neutron detection, it is not possible to use PSD [12, 19, 22, 23].

Table 1. The cross-section σ_a of thermal neutron radiative capture for some isotopes [12 (p. 402)]

Isotope	Cross-section of thermal neutron absorption, Barn	Natural abundance (%)
^{3}He	5.4×10^3	0.000137
^{6}Li	0.9×10^3	7.59
^{10}B	3.8×10^3	19.9
^{113}Cd	2×10^3	12.22
^{155}Gd	6×10^4	14.8
^{157}Gd	2.5×10^5	15.65

There is a rather effective way of solving this problem. A scintillation material, which developed to detect thermal neutrons, has to have the very high efficiency of this process. Table 1 demonstrates the thermal neutron capture cross-sections and natural abundance of some the most promising isotopes for thermal neutrons detection. Thus, the most promising are Gd-bearing materials because the cross-section of thermal neutron detection and natural abundance of isotopes ^{155}Gd and ^{157}Gd are too high. Below we focus on the results obtained for such the materials, because in that way we obtained enough effective material, even if it is very thin. A thin sample has a low efficiency of detection of photons of gamma radiation. This is the principle of selective registration of thermal neutrons, which we will use below.

If gadolinium captures a thermal neutron it can leads to the emission of conversion electrons (33 keV), characteristic X-rays (44 keV), and cascades of high-energy photons of gamma radiation (about 8 meV). The total effect of emission of conversion electrons and Gd K X-rays may cause the total 77 keV scintillation peak formation [5, 24]. The probability of generation of the 33 keV conversion electrons per one captured neutron is about 0.65 and the probability to observe 77 keV peak is about 0.39 [24]. Below we will analyse this idea on the example of the composite scintillators based on the grains of cerium-doped gadolinium silicate Ce:Gd_2SiO_5 (Ce:GSO) and gadolinium pyrosilicate Ce:$Gd_2Si_2O_7$ (Ce:GPS) scintillation materials, which are sensitive to background gamma radiation.

The aim of this work is an overview of our achievements in the creation of new scintillation materials, namely, composite scintillators and analysis of their potential as detectors of neutron fluxes of low intensity.

2 Technologies

To grow the stilbene and *p*-terphenyl organic single crystals we use the Bridgman-Stockbarger technique [12 (p. 25), 23]. According to [25], the light yield (LY) of the single crystals of stilbene, undoped *p*-terphenyl, and doped by 1,4-diphenyl-1,3-butadiene *p*-terphenyl is about 14,700, 17,000, and 24,900 photons per 1 meV, respectively.

The preparation technology of organic composite detectors includes the following stages: (i) purification of the raw material (we used the method of oriented crystallization, when randomly oriented crystalline grains arise inside a boule); (ii) self-cracking of the boule under a layer of liquid nitrogen (the boule obtained on step (i) cracks along the grains boundaries and the need in the stage of growth of the single crystal disappears); (iii) to select the grain fractions of required sizes we sieve the grains using the calibrated sieves; (iv) drying of the grains (during 24 h); (v) preparation of the two-component organosilicone dielectric gel; (vi) introduction of the grains into the gel in the ratio 70 and 30 weight %, respectively; (vii) mixing the crystalline grains and the gel; (viii) introduction the composition into a housing made from acrylic plastic (light guide material); (ix) vacuum treatment of the scintillation composition (during 30 min); (x) polymerization of the sealed scintillation composition (during 48 h); (xi) application a diffusive reflecting material [e.g. Tetratek (polytetrafluoroethylene)] on the housing (more detailed information can be found in our works [13, 14, 26–29]).

Ce:GSO and Ce:GPS crystals were grown by the Czochralski technique. To produce a composite scintillator we crush the offal of the crystal growth and of the crystal tooling. The concentration of Ce in Ce:GSO and Ce:GPS was about 0.5 mol. % and 7 mol. %, respectively. The LY of Ce:GSO crystals is 12,500 photons/MeV [28]. The authors [30] have shown that this value changes appreciably with the cerium concentration in the crystals. The authors [31] obtained that the LY of Ce:GPS has to be from 30,000 to 40,000 photons/MeV.

Thus, a composite scintillator consists of the grains the typical size L of which is between $d_i < L < d_j$, where d_i and d_j is the mesh dimension of the calibrated sieves i and j. Here and further, we will use such the values L, which are equal to the averaged values of the grains $L_{av} = (d_i + d_j)/2$.

3 Experimental

In our following experiments, we detected the scintillation pulses using a 9272B photomultiplier tube (ET Enterprises [32]). We chose radionuclide sources of ^{239}Pu–Be and ^{252}Cf as the sources of fast neutrons. In the same time, they are the sources of gamma radiation. We obtained the recoil proton spectra not distorted by accompanying

gamma radiation using PSD. As the source of alpha particles was selected a ^{239}Pu radionuclide source (5.15 meV) and the source of gamma radiation photons was a ^{137}Cs radionuclide source (0.662 meV). We used them to study the LY of composite scintillators. As the reference detector, we used the single crystals of the same chemical composition.

To test Gd-bearing single crystals and composite scintillators based on their grains as thermal neutron detectors we used a radionuclide ^{239}Pu–Be source with neutron flux 1×10^5 neutrons per second. We placed it inside a calibrated paraffin sphere (15 cm in diameter) to moderate fast neutrons. As the result, this paraffin sphere moderates the part of fast neutrons $\eta_{th} = 9\%$ to the energy of thermal neutrons. The rest of the neutrons of higher energies and photons of gamma radiation accompany these thermal neutrons when they leave the paraffin sphere. The ^{239}Pu–Be source emits about three gamma radiation photons per one neutron. Therefore, to reduce direct irradiation of the samples by low energy photons of gamma radiation we used the 25 mm thick lead. The difference in the number of scintillations measured during the same time interval with and without the plate of cadmium 1.3 mm thick identifies the thermal neutron events.

The calibration procedure of the linearity of the set-up was done using the Compton edge energies of the gamma lines E_γ for the following radionuclide sources: ^{22}Na, ^{60}Co, ^{137}Cs, ^{152}Eu, ^{241}Am as well from the ^{12}C(n, γ) reaction in a ^{239}Pu–Be radionuclide source. The light output of the scintillators relative to gamma energy E_γ was linear to within 5%.

3.1 Fast Neutron Detectors

Below we will demonstrate the possibilities of composite scintillators to detect fast neutrons on example of a series of 10 composite detectors (diameter D = 30 mm and high h = 20 mm) obtained from stilbene crystalline grains of different fractions, and analogous series of 10 composite detectors based on p-terphenyl doped with 1,4-diphenyl-1,3-butadiene. The following linear sizes L of grains were used: 1.0–1.2, 1.2–1.5, 1.5–1.7, 1.7–2.0, 2.0–2.2, 2.2–2.5, 2.5–3.0, 3.0–3.5, 3.5–4.0, 4.0–4.5 mm.

In our investigations, we often use such the approach when the series of composite detectors with different grain sizes L are studied. The reason is the following. Unlike the single crystal of a given composition, the properties of a composite scintillator are determined not only by it sizes, but by another independent parameter, namely, the size of the grains inside the scintillator (see e.g. [13, 14, 17, 18, 21, 23, 26–28, 33]).

Figures 2 and 3 shows the LY and relative light output (LO), respectively, for each fraction of the grains (different L_{av}) of the composite scintillators containing grains of doped p-terphenyl [13]. Figure 2 represents the LY-values in absolute units for the case of excitation by photons of gamma-radiation. Figure 3 demonstrates the relative values of LO as a percentage for the excitation by short-range alpha particles. The LO of a standard doped p-terphenyl single crystal we designate as 100%. Figure 3 shows that the LO reaches the maximum at $L_{av} \sim 2.5$ mm and practically does not change with further increase of the L_{av} value.

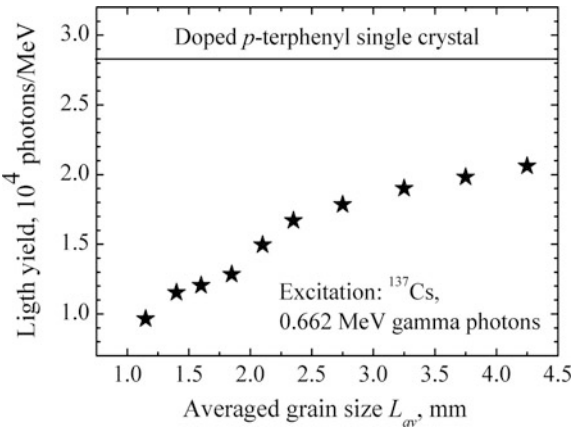

Fig. 2. The light yield of composite scintillators containing grains of doped *p*-terphenyl of various sizes (L_{av}) obtained when irradiated by 0.662 meV photons of gamma radiation [13]

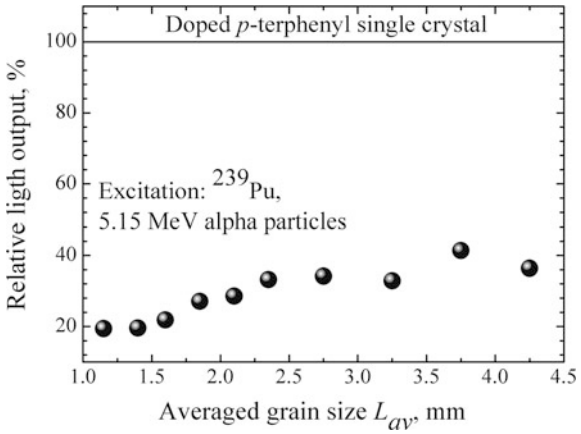

Fig. 3. The relative light output of composite scintillators containing grains of doped *p*-terphenyl of various sizes (L_{av}) obtained when irradiated by 5.15 meV alpha particles [13]

To determine the heterogeneity of the composite scintillators we measured the scintillation signal at different points of the samples of large diameter ($d = 200$ mm, $h = 20$ mm). The measurements show the spread of the LO-values for different parts of these detectors does not exceed the standard error of the method of the LO measurements (5%). Thus, the technique gives reproducible results and allows us to make the homogeneous large-diameter composite detectors. For details, please turn to the quoted works [13–15, 34].

The relative efficiency ε of ^{252}Cf fast neutron detection by the composite scintillators based on stilbene crystalline grains reports the paper [28]. According to [28], the fraction of crystalline grains with sizes L from 1.7 to 2.2 mm is optimal to prepare the

composite scintillator that is effective to detect ^{252}Cf fission neutrons. It agrees with the results of studies of composite detectors irradiated by a ^{239}Pu–Be source of fast neutrons (see e.g. [13, 14, 23, 26, 27]). The scintillation efficiency may strongly depend on the grain size. This is because the charge states recombination results in the formation of excited states and their subsequent luminescence. The sequence of these processes is more effective when they take place in one the same grain. It is possible when the track length of an ionizing particle (the track of a recoil proton in our case) does not exceed the linear size of a single grain.

Table 2 demonstrates the relative efficiency of fast neutron detection ε for a series of stilbene composite detectors (D = 32 mm, L is from 1.7 to 2.2 mm) of different height h irradiating by fast fission neutrons of ^{252}Cf. For each of the composite detector the organic single crystal of the identical size plays the role of a "reference" detector. Table 2 shows that the ε-value slightly decreases with the height h growth. The light scattering in the multilayer scintillation material is the main cause of this effect. One can see the difference between the experimental value of the relative efficiency of fast neutron detection $\varepsilon \sim$ 0.5–0.6 and its theoretical value ($\sim$0.7) determined by the concentration of the scintillating material (stilbene) in the gel base (Sylgard-527). It is the result of the joint action of light scattering and the additional losses of the recoil proton energy in the non-scintillating gel base.

Table 2. The relative efficiency of fast neutron detection ε of ^{252}Cf for stilbene composite detectors versus their height h

Detector height h (mm)	The relative efficiency ε
2	0.569 (±0.085)
3	0.556 (±0.083)
5	0.450 (±0.067)
7	0.562 (±0.084)
10	0.611 (±0.092)
15	0.503 (±0.075)
20	0.435 (±0.065)

In [15, 34, 35] it was shown that the composite detectors based on organic crystalline grains have high PSD capability so as the single crystals. In [35] for the case when ^{239}Pu–Be source irradiates the samples of organic detectors it was obtained that the value of figure-of-merit (FOM) for the experimental set-up with the neutron energy threshold of 1 meV is equal to 2.41 ± 0.21 for the reference stilbene single crystal (D = 30 mm, h = 10 mm). For the stilbene composite detector with D = 50 mm and h = 25 mm FOM is 1.89 ± 0.13 and for stilbene composite detector with D = 50 mm and h = 50 mm FOM is 1.38 ± 0.09. Thus, the values of FOM obtained for thin composite scintillators are only slightly poorer than FOM for the stilbene single crystal. For thicker composite scintillators FOM is lower, because of the lower light output caused by stronger light absorption inside the scintillator. Additionally, we studied the values of FOM for the case of irradiation by fast neutrons of ^{252}Cf [15]. The FOM of the composite stilbene scintillator (D = 50 mm and h = 10 mm) was evaluated as 80%

against that of the stilbene single crystal scintillator (D = 25 mm and h = 20 mm). The FOM of the large-area composite stilbene scintillator (D = 200 mm and h = 20 mm) was evaluated as about 75%, against that of the stilbene single crystal scintillator (D = 50 mm and h = 40 mm).

3.2 Thermal Neutron Detectors

To obtain thermal neutron detectors we studied the single crystals of Ce:GSO and Ce:GPS as well as composite scintillators based of their grains. For details, please turn to the [17–19, 33].

Figure 4 demonstrates typical thermal neutron scintillation spectra of the Ce:GPS single crystal. Curve 1 in Fig. 4 is the scintillation spectrum of the Ce:GPS single crystal obtained during the irradiation by neutrons and photons of gamma-radiation those leave the paraffin sphere with the ^{239}Pu–Be source inside it. Subtraction of curve 2 from curve 1 gives a curve with two distinct maxima in the region of 33 and 77 keV. Such a curve will be given later (see Fig. 6), when discussing the properties of the combined detector of fast and thermal neutrons. Note that these resulting curves are similar and differ only in the contribution of the peaks at 33 and 77 keV. Let us take the contribution the value of the maximum of the peak with the energy of 77 keV as 100%. In such the case one can obtain that the contribution of the 33 keV peak decreases from 226 to 102% and from 220 to 104% when the grain size increases from $L < 0.06$ mm up to L = 0.3–0.5 mm for the composite scintillators containing the grains of Ce:GSO and Ce:GPS, respectively. For higher values of L these peaks are not separated and appear as one peak. In the same time for single crystals of the same thickness, this value is less than 100%. The single-layer composite scintillators have the best neutron-to-gamma ratio.

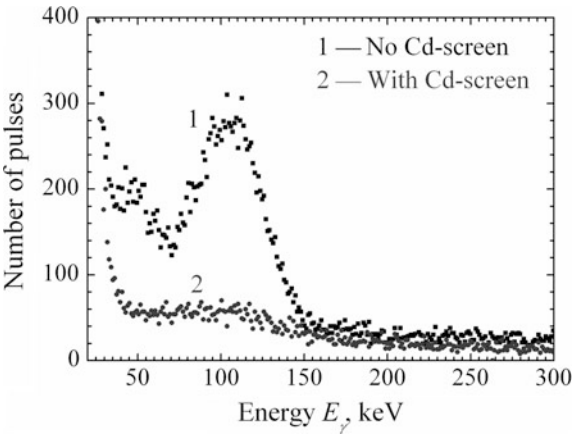

Fig. 4. The amplitude spectra of the Ce:GPS single crystal were obtained without (curve1) and with (curve 2) the Cd-screen

3.3 Combined Detector for Separate Detection of Fast and Thermal Neutrons in the Presence of Background Gamma Radiation

In [17] we showed the possibility to use composite scintillators to create a combined scintillator for separate detection of thermal and fast neutrons in the presence of gamma-background. In the works [18, 29, 33] we returned to this idea.

The scintillator, which detect fast neutrons, contains crystalline grains of stilbene with size L_S from 2.5 to 3.0 mm. The other part of the combined scintillator that detects thermal neutrons is a single-layer composite scintillator containing Ce:GPS or Ce:GSO crystalline grains. This composite scintillator is thin enough to reduce appreciably a gamma background of high and medium energies. We run the measurements for the cases when this single-layer composite scintillator contained one of three types of grains, namely, grains with average sizes from 0.06 to 0.1, from 0.1 to 0.3 and from 0.3 to 0.5 mm (see Table 3). Both the scintillators were inside a cylindrical plastic housing. An additional plastic plate 2 mm thick separates the scintillators. The combined detectors are 30 mm in diameter D and 20 mm in high h. In a real experiment, the combined detector must have the additional shielding, witness detector or their combination [17]. Figure 5 shows the schematic diagram of such the combined detector (the plastic plate is not shown).

Table 3. The ε_{th}-value of the combined detectors consisting of Ce:GPS scintillator with different L_{GPS} and the composite scintillator on the base of stilbene grains with L_S from 2.5 to 3.0 mm

Energy range (keV)	L_{GPS} (mm)		
	0.06–0.1	0.1–0.3	0.3–0.5
20–55	0.182	0.122	0.175
56–120	0.291	0.342	0.348
20–120	0.473	0.464	0.523

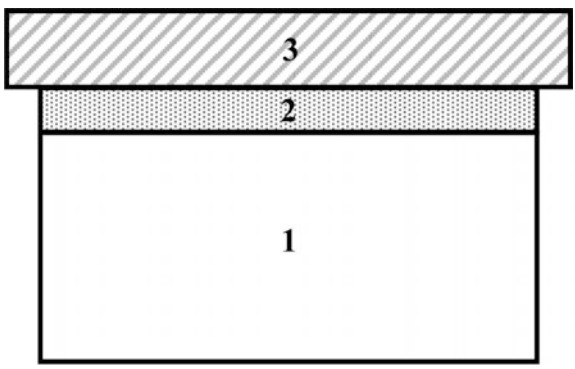

Fig. 5. Schematic diagram of a combined detector: 1 is a fast neutron detector, 2 is a detector of thermal neutrons, 3 is a shielding material

Figure 6 demonstrates the spectrum of thermal neutrons which we obtain using the combined detector that consists of two composite scintillators including the grains of (i) stilbene (L_S = 2.5–3.0 mm) and (ii) Ce:GPS (L_{GPS} = 0.1–0.3 mm). The bottom X-axis is calibrated in terms of scintillation amplitudes of the Ce:GPS composite scintillator that was excited by photons of gamma radiation with energies E_γ^{GPS}. The top X-axis we calibrated in the number of scintillation photons. The solid line 1, 2 and 3 shows the bounders of the energy ranges, in which we analyse the signal (see Fig. 6) [13, 17]. Note that the end of the scintillation signal corresponds to 7 × 10^2 photons.

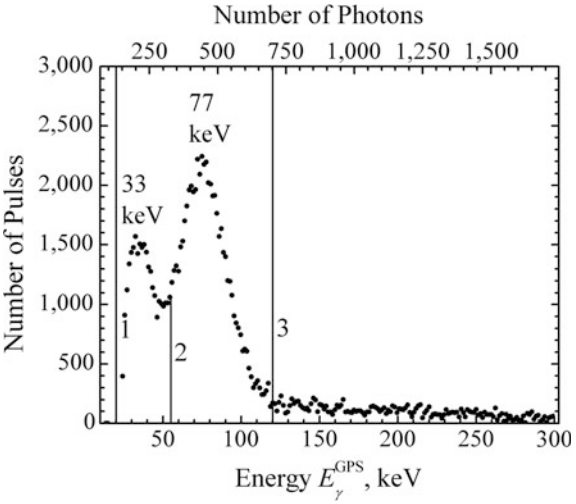

Fig. 6. Scintillation amplitude spectrum obtained at excitation by thermal neutrons of the combined detector consisting of two composite scintillators: based on grains of stilbene (L_S = 2.5–3.0 mm) and the grains of the Ce:GPS (L_{GPS} = 0.1–0.3 mm)

Figure 7 shows the reconstructed neutron spectrum of the ^{239}Pu–Be source which we obtain using the combined detector that consists of two composite scintillators including grains of stilbene (L_S = 2.5–3.0 mm) and Ce:GPS (L_{GPS} = 0.1–0.3 mm [13, 17]. Figure 7 represents known quantities of fast neutron energies which are reported in theoretical and experimental papers (see e.g. [12 (pp. 386–387), 13]), namely, 3.1, 4.2, 4.9, 6.4, 6.7, 7.3, 7.9, 8.6 and 9.7 meV. The numbers 1–9, respectively, denote these energies.

On the top X-axis one can see the number of scintillation photons match the scintillation signal. We calibrated the energy scale (X-axis) in scintillation photons, i.e. in terms of the LY of the reference stilbene single crystal. The neutron measurements we run after the calibration and for the same measuring conditions. The beginning of the neutron signal corresponds to (1.3–1.4) × 10^4 photons. Thus, the magnitude of the maximum signal in the scintillation spectrum obtained from thermal neutrons (10^2 photons) and minimal signal obtained from fast neutrons after PSD (10^4 photons). It

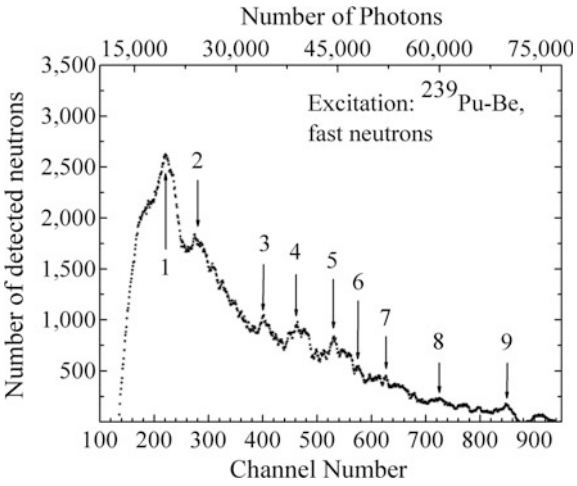

Fig. 7. The reconstructed neutron spectrum of ^{239}Pu–Be source for the combined detector consisting of two composite scintillators: based on grains of stilbene (L_S = 2.5–3.0 mm) and the grains of the Ce:GPS (L_{GPS} = 0.1–0.3 mm)

lays the physical basis for the separate registration of thermal and fast neutrons by such the combined scintillator. These signals can be recorded in different energy windows.

As it was noted above, for a good separation of the signals from thermal neutrons and gamma background, it is necessary that the composite detector of thermal neutrons was thin. Reducing the thickness of the detector can lead to loss of effectiveness of the registration. The following is the assessment of the efficiency of registration of the composite scintillator containing grains of Ce:GPS or Ce:GSO working together with the composite scintillator on the base of stilbene grains.

Let N_Σ denotes the number of events of thermal neutron detection. Then in the general case, the efficiency of thermal neutron detection ε_{th} is

$$\varepsilon_{th} = \frac{N_\Sigma}{t \cdot F_{fast} \cdot \eta_{th} \cdot \frac{S}{4\pi R^2}},$$

were t is the time of accumulation of these events, F_{fast} is the fast neutron flux (in our case it is 1×10^5 neutrons per second), η_{th} is the fraction of thermal neutrons obtained by the moderation of fast neutrons per one fast neutron (0.09), S is the thermal neutron detector area, R is the distance between the source and the detector.

Table 3 shows the ε_{th}-value for the combined detectors consisting of Ce:GPS scintillator with different L_{GPS} and the composite scintillator on the base of stilbene grains with L_S from 2.5 to 3.0 mm for the three energy ranges of scintillation spectra.

4 Conclusions

Above we discuss the scintillation characteristics of the composite scintillators as fast and thermal neutrons detectors. The proposed technologies create the new opportunities to obtain large-diameter composite scintillators for detection of short-range ionizing radiation, thermal neutrons, and spectrometry of fast neutrons.

For composite scintillators those include the stilbene grains the fast neutron detection efficiency is about 50–55% with respect to organic single crystals of the same size. The single-layer composite scintillators with the Ce:GSO or Ce:GPS crystalline grains less than 0.1 mm provides detection of thermal neutrons by registration of scintillation pulses of 33 keV conversion electrons (the energy range 20–55 keV) with efficiency $\varepsilon_{th} \sim 20\%$. The simultaneous detection of scintillation pulses from the conversion electrons (33 keV) and the conversion electrons accompanied by Gd K X-rays (77 keV) enables to obtain the ε_{th}-values 40–50% in the range from 20 to 120 keV. The combined composite detector can separately detect thermal and fast neutrons in the presence of gamma background in different ranges of light intensities (up to 10^2 photons and from 10^4 photons, respectively). If the electronics is linear over a wide dynamic range then it becomes possible to analyse separately the signals from fast and thermal neutrons in two different amplitude bands.

The composite and combined composite scintillation detectors are non-hygroscopic, effective scintillation materials of thermal and fast neutrons as well as for detection such short-range radiations as alpha particles. They have no technological limitation on theirs shape and on the area of theirs input window.

References

1. Ann ICRP, The 2007 recommendations of the international commission on radiological protection. Publ. 103. Ann ICRP **37**(2–4),1–332 (2007)
2. F.D. Brooks, R.W. Pringle, B.L. Funt, Pulse shape discrimination in a plastic scintillator. IRE Trans. Nucl. Sci. **7**(2–3), 35–38 (1960)
3. J.B. Birks, *The Theory and Practice of Scintillation Counting* (Pergamon Press, London, 1967)
4. M. Moszynski, G.J. Costa, G. Guillaume et al., Study of n-γ discrimination with NE213 and BC501A liquid scintillators of different size. Nucl. Instrum. Meth. A **350**(1–2), 226–234 (1994)
5. Z.W. Bell, G.M. Brown, C.H. Ho, F.V. Sloop, Organic scintillators for neutron detection. Proc. SPIE **4784**, 150–163 (2003)
6. S.A. Pozzi, J.A. Mullens, J.T. Mihalczo, Analysis of neutron and photon detection position for the calibration of plastic (BC-420) and liquid (BC-501) scintillators. Nucl. Instrum. Meth. A **524**(1–3), 92–101 (2004)
7. L. Swiderski, M. Moszynski, D. Wolski et al., Boron-10 loaded BC523A liquid scintillator for neutron detection in the border monitoring. IEEE Trans. Nucl. Sci. **55**(6), 3710–3716 (2008)
8. G. Hull, N.P. Zaitseva, N.J. Cherepy, New organic crystals for pulse shape discrimination. IEEE Trans. Nucl. Sci. **56**(3), 899–903 (2009)

9. T. Szczęśniak, M. Moszyński, A. Syntfeld-Każuch et al., Light pulse shapes in liquid scintillators originating from gamma-rays and neutrons. IEEE Trans. Nucl. Sci. **57**(6), 3846–3852 (2010)
10. N. Zaitseva, B.L. Rupert, I. Pawelczak et al., Plastic scintillators with efficient neutron/gamma pulse shape discrimination. Nucl. Instrum. Meth. A **668**, 88–93 (2012)
11. S.A. Pozzi, M.M. Bourne, S.D. Clarke, Pulse shape discrimination in the plastic scintillator EJ-299-33. Nucl. Instrum. Meth. A **723**, 19–23 (2013)
12. N.Z. Galunov, V.P. Seminozhenko, *Radioluminescence of Organic Condensed Media* (Naukova Dumka, Kyiv, 2015). [in Russian]
13. N.L. Karavaeva, O.A. Tarasenko, Development of new composite scintillators based of organic single crystal grains. Funct. Mater. **16**(1), 92–96 (2009)
14. N.Z. Galunov, B.V. Grinyov, N.L. Karavaeva et al., Development of new composite scintillation materials based on organic crystalline grains. IEEE Trans. Nucl. Sci. **56**(3), 904–910 (2009)
15. S.K. Lee, J.B. Son, K.H. Jo et al., Development of large-area composite stilbene scintillator for fast neutron detection. J. Nucl. Sci. Technol. **51**(1), 37–47 (2014)
16. J.H. Baker, N.Z. Galunov, O.A. Tarasenko, Variation of scintillation light yield of organic crystalline solids for different temperatures. IEEE Trans. Nucl. Sci. **55**(5), 2736–2738 (2008)
17. N.L. Karavaeva, Combined composite scintillation detector or separate measurements of fast and thermal neutrons. Funct. Mater. **17**(4), 549–553 (2010)
18. N.L. Karavaeva, Composite scintillators as new type of a scintillation material. Probl. At. Sci. Technol. **93**(5). Series: Nuclear Physics Investigations 63, 91–97 (2014)
19. J.H. Baker, N.Z. Galunov, A.M. Stepanenko, O.A. Tarasenko, Some aspects of discrimination techniques for the measurement of neutrons and photons of gamma radiation in geological applications. Radiat. Meas. **38**(4–6), 817–820 (2004)
20. C.W.E. van Eijk, A. Bessière, P. Dorenbos, Inorganic thermal-neutron scintillators. Nucl. Instrum. Meth. A **529**(1–3), 260–267 (2004)
21. N.Z. Galunov, B.V. Grinyov, N.V. Karavaeva et al., Gd-bearing composite scintillators as the new thermal neutron detectors. IEEE Trans. Nucl. Sci. **58**(1), 339–346 (2011)
22. J.H. Baker, N.Z. Galunov, V.G. Kostin et al., A technique for the selective detection of neutrons in geological applications. Probl. At. Sci. Technol. **51**(5). Series: Nuclear Physics Investigations 48, 126–130 (2007)
23. N.Z. Galunov, S.V. Budakovsky, N.L. Karavaeva et al., New effective organic scintillators for fast neutron and short-range radiation detection. IEEE Trans. Nucl. Sci. **54**(6), 2734–2740 (2007)
24. J. Haruna, J.H. Kaneko, M. Higuchi et al., Response function measurement of Gd2Si2O5 scintillator for neutrons. In: *Proceedings of IEEE Nuclear Science Symposium Conference Record*, Honolulu, Hawaii, 27 October–3 November 2007
25. N.Z. Galunov, O.A. Tarasenko, Effect of polarization on recombination of charge states in an ionizing particle track in organic molecular crystals. Mol. Cryst. Liq. Cryst. **606**(1), 176–188 (2015)
26. S.V. Budakovsky, N.Z. Galunov, B.V. Grinyov et al., Stilbene crystalline powder in polymer base as a new fast neutron detector. Radiat. Meas. **42**(4–5), 565–568 (2007)
27. N.Z. Galunov, B.V. Grinyov, J.K. Kim et al., Novel fast neutron detectors for environmental and security applications. J. Nucl. Sci. Technol. **5**, 367–370 (2008)
28. O. Tarasenko, N. Galunov, N. Karavaeva et al., Stilbene composite scintillators as detectors of fast neutrons emitted by ^{252}Cf. Radiat. Meas. **58**, 61–65 (2013)
29. N.Z. Galunov, O.A. Tarasenko, V.A. Tarasov, Optical and scintillation properties of stilbene polycrystalline and composite materials. Funct. Mater. **22**(1), 61–68 (2015)

30. M. Balcerzyk, M. Moszynski, M. Kapusta et al., YSO, LSO, GSO and LGSO. A study of energy resolution and nonproportionality. IEEE Trans. Nucl. Sci. **47**(4), 1319–1323 (2000)
31. S. Kawamura, J.H. Kaneko, M. Higuchi et al., Floating zone growth and scintillation characteristics of cerium-doped gadolinium pyrosilicate single crystals. IEEE Trans. Nucl. Sci. **54**(4), 1383–1386 (2007)
32. ET Enterprises, 9272B series data sheet. Available: https://my.et-enterprises.com/pdf/9272B.pdf
33. N.Z. Galunov, B.V. Grinyov, N.L. Karavaeva et al., Combined composite scintillation detector for separate measurements of fast and thermal neutrons. In: *Proceedings of IEEE Nuclear Science Symposium Conference Record*, Knoxville, Tennessee, 30 October–6 November 2010
34. S.K. Lee, Y.H. Cho, B.H. Kang et al., Scintillation properties of composite stilbene crystal for neutron detection. Prog. Nucl. Sci. Technol. **1**(1), 292–295 (2011)
35. J. Iwanowska, L. Swiderski, M. Moszynski et al., Neutron/gamma discrimination properties of composite scintillation detectors. J. Instrum. **6**(7007), 1–10 (2011)